Development of an EPICS-based Automatic Superconducting Module Test System for SHINE

Authors: Mr. Chen Luo, Xu, Mr. Kai, Li, Dr. Zheng, Dr. Ya-Wei Huang, Zhai, Dr. YF, Wu, Hailong, Hong Wu, Liu, Mr. Xu-ming, Mr. Xiao-han Ou-yang, Mr. Zhenyu Ma, Huang, Xuefang, Hong-ru Jiang, Zhang, Zhi-Gang, Yang, Wenfeng, Chan, Mr. Qiang, Li, Xin-yu, Zheng, Dr. Xiang, Lei Gao, Zhao, Yu-Bin, Zhao, Mr. Shen-jie, Zhao, Shenjie

Date: 2025-11-21T00:00:00+00:00

Abstract

The Shanghai High Repetition Rate XFEL and Extreme Light Facility (SHINE) is a high-frequency hard X-ray free-electron laser (FEL) facility with a maximum repetition rate of 1 MHz, delivering photon energy from 0.4 to 25 keV. A critical component of SHINE is the superconducting module. Given the complexity of its internal components and structure, rigorous and precise evaluation of its performance is essential prior to installation. To evaluate its performance, we developed an automated module test system based on the Experimental Physics and Industrial Control System (EPICS). This comprehensive test system integrates various key technical domains, including radio frequency (RF), cryogenics, vacuum, electronics, radiation, and control. The test control framework employs simple network management protocol (SNMP) for software architecture, StreamDevice for standardized device driver access, PyDM for user interface, network time protocol (NTP) for timing synchronization, and Python scripting for test automation. The test system has been successfully applied to test multiple superconducting modules at our institute. This automation significantly reduces testing time and simplifies procedures, standardizes procedural execution, ultimately enhances the overall test consistency and efficiency, while also providing data acquisition that beam operation data analysis.

Full Text

Development of an EPICS-based Automatic Superconducting Module Test System for SHINE

Chen Luo, Kai Xu, Zheng Li,[1] Ya-wei Huang,[2] Yan-fei Zhai, Hailong Wu, Hong Wu, Xu-ming Liu, Xiao-han Ou-yang, Zhen-yu Ma,

Xue-fang Huang, Hong-ru Jiang, Zhi-gang Zhang, Wen-feng Yang, Qiang Chang, Xin-yu Li,[1] Lei Gao,[3] Xiang Zheng, Yu-bin Zhao,[1] and Shen-jie Zhao[1]

[1]Shanghai Advanced Research Institute, Chinese Academy of Sciences, Shanghai 201210

[2]ShanghaiTech University, Shanghai 201210

[3]Shanghai Apactron Particle Equipment Co. Ltd, Shanghai 201815

Abstract

The Shanghai High Repetition Rate XFEL and Extreme Light Facility (SHINE) is a high-frequency hard X-ray free-electron laser facility with a maximum repetition rate of 1 MHz, delivering photon energies from 0.4 to 25 keV. A critical component of SHINE is the superconducting module. Given the complexity of its internal components and structure, rigorous and precise evaluation of its performance is essential prior to installation. To evaluate its performance, we developed an automated module test system based on the Experimental Physics and Industrial Control System (EPICS). This comprehensive test system integrates various key technical domains, including radio frequency (RF), cryogenics, vacuum, electronics, radiation, and control.

The test control framework employs the Simple Network Management Protocol (SNMP) for software architecture, StreamDevice for standardized device driver access, PyDM for the user interface, the Network Time Protocol (NTP) for timing synchronization, and Python scripting for test automation. The test system has been successfully applied to test multiple superconducting modules at our institute. This automation significantly reduces testing time and simplifies procedures, standardizes procedural execution, ultimately enhances overall test consistency and efficiency, while also providing data acquisition for beam operation data analysis.

Keywords: SHINE · EPICS · Module Test · RF Test · Automation

INTRODUCTION

The Shanghai High Repetition Rate XFEL and Extreme Light Facility (SHINE) is currently under construction and is designed to be a high-repetition-rate hard X-ray facility. The facility consists of a linear accelerator section, two undulators, two beamlines, four cryogenic stations, and other supporting infrastructure. The linear accelerator is divided into five sections (L0–L4). Beamline FEL-1 provides photon energies from 3.0–15.0 keV, while beamline FEL-2 delivers photon energies from 0.2–3.0 keV. The cryogenic station includes three 4 kW cooling capacities at 2 K for the SHINE tunnel and 1 kW cooling capacities at 2 K for the test halls. The general layout of SHINE is shown in Fig. 1 [FIGURE:1].

Central to its design is the accelerator based on superconducting radio-frequency (SRF) technology, requiring the mass production and precise evaluation of numerous superconducting cryomodules. The injector section (L0) comprises one twin-FPC cavity module (i1CM) and one nine-cell cavity module (i8CM). The L1 section includes two 1.3 GHz modules and two 3.9 GHz modules, while the L2–L4 sections comprise 52 1.3 GHz modules [1, 2]. Each module includes eight superconducting cavities, eight fundamental power couplers (FPC), eight tuning devices, sixteen HOM couplers, one cryomodule system (including thermostat, vacuum pipe system, and vacuum vessel), a beam position monitor (BPM), a superconducting magnet, and a support system [3, 4]. The layout of the module is presented in Fig. 2 [FIGURE:2].

Before assembly, cavities are tested in both bare and dressed states through vertical tests (VT), and only qualified cavities are assembled into modules. One module requires over 20 days of testing, and only those meeting specifications are installed in the SHINE tunnel. The assembly and testing of modules are conducted in two halls on the campus of the Shanghai Advanced Research Institute, which have a combined area of 3,000 square meters. These halls are equipped with four vertical test platforms (VTF1/2 in ATF1 and VTF3/4 in ATF2) and four horizontal test platforms (HTF1/2 in ATF1 and HTF3/4 in ATF2). The layout of the halls is shown in Fig. 3

. The facility can assemble and test three modules per month and has already completed more than twenty module assemblies and tests.

The module test platforms include radiation protection, vacuum, cryogenics, power sources, low-level RF (LLRF), RF interlocks, RF test, BPM, and superconducting magnets. The module test objectives are to verify: (1) whether all components of the module meet design requirements; (2) whether the assembly process meets specifications; and (3) whether the module meets beam operational requirements for installation in the tunnel.

EPICS is a control system developed by Los Alamos National Laboratory (LANL) and Argonne National Laboratory (ANL) [5, 6]. EPICS is a standard model known for portability, expansion, and reusability, and has been applied in hundreds of physics experimental facilities, such as the Beijing Electron-Positron Collider (BEPC), Shanghai Synchrotron Radiation Facility (SSRF), Linac Coherent Light Source (LCLS), and others.

The stringent operational requirements of SHINE, particularly its high repetition rate, demand that each superconducting module operate within extremely tight tolerances. Manual module testing procedures are time-consuming, prone to human error, and struggle to ensure high repeatability across a large number of modules. To mitigate these challenges and ensure quality assurance, an integrated and fully automated test solution is crucial. This paper describes the design and implementation of an EPICS-based control system developed specifically for module testing. The system adopts reliable scripting to achieve standardized device access, test execution, and real-time data archiving.

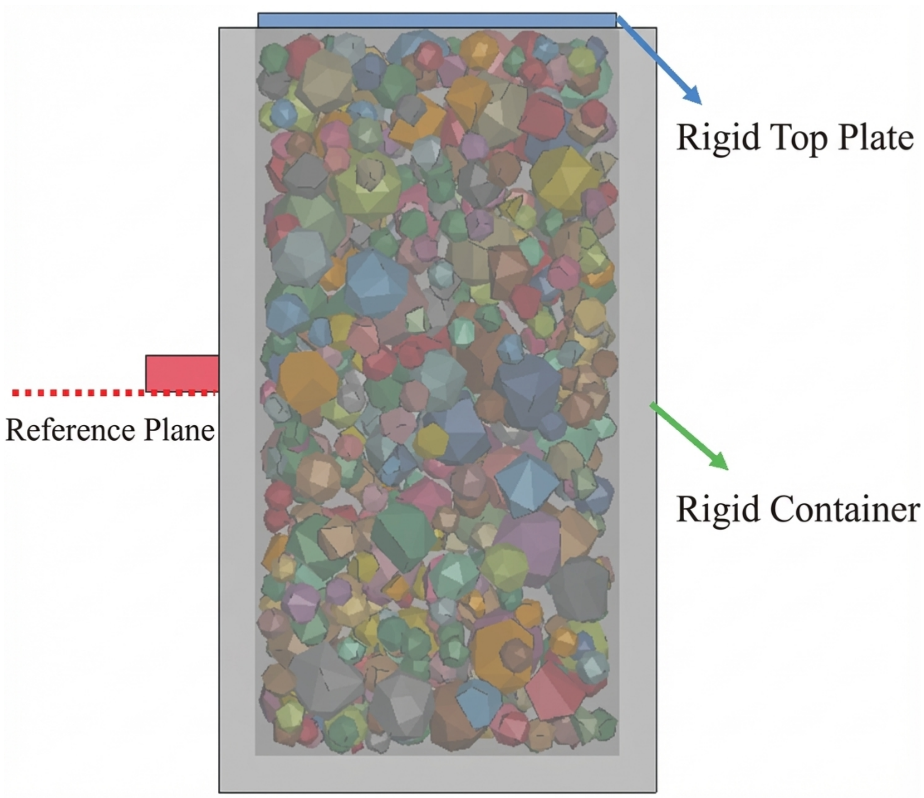

Figure 1: Figure 3

II. MODULE TEST REQUIREMENTS AND IMPLEMENTATION

A. Module Test Requirements

The module test objectives are defined by SHINE acceptance criteria, covering accelerating gradient, heat load, high-order mode (HOM), tuner performance, quadrupole magnet, BPM, cryomodule, and vacuum [7, 8]. The acceptance criteria are illustrated in Table 1 [9]. Specific requirements include measurement of the superconducting cavity spectrum and π-mode frequency; characterization of FPC conditions at room temperature and 2 K [10]; determination of the external quality factor of the FPC (Qe); cavity performance tests including Eacc vs Q0, Eacc vs X-ray, and Eacc vs dark current; and automatic generation of test reports from raw data.

B. Implementation of the Module Test Platform

The module test platform involves numerous integrated systems, as illustrated in Fig. 4

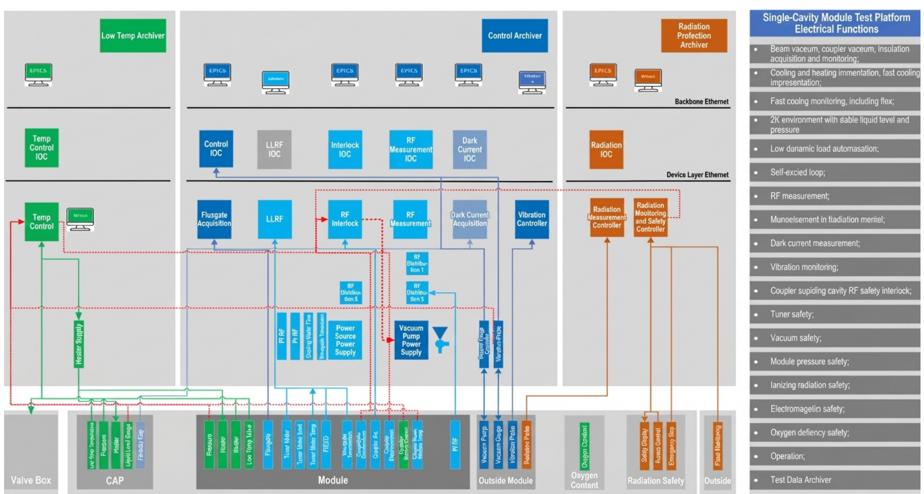

Figure 2: Figure 4

. The platform integrates: (1) a solid-state power amplifier (SSA) that provides cavity power with a maximum output of 5.2 kW, connected to the FPC through a waveguide; (2) LLRF that controls forward and feedback signals of the cavity via an FPGA-based loop, allowing the cavity to achieve resonance through the Self-Excited Loop (SEL) [11]; (3) RF interlocks that protect the cavity and FPC by monitoring quench, temperature, electronics, and other protection signals to shut down the SSA during faults; (4) radiation monitoring using a Geiger–Müller counter positioned two meters from the center of the cavity; (5) dark current measurement with Faraday cups at both ends of the module (feedcap and endcap), capable of detecting nanoampere-scale currents generated by radiation; (6) cryomodule regulation through valves and heaters to control liquid helium levels and pressure, where static load is calculated from heater power and flowmeter rate while dynamic load is derived from applied RF power and flowmeter measurements [12–14].

During module testing, RF testing constitutes the primary task and occupies the entire test period. Each cavity has four ports: one input power port (Pf), one extraction power port (Pt), and two HOM ports (homC and homP). The system measures power values from eight cavities: PF, PR, PT, PhomC, and Phompu, totaling 40 values. The cavity acceleration gradient at the resonant frequency and the loaded quality factor are also determined. For long-term operation and to account for heating effects in the FPC, we use formula (2) to calculate Eacc based on PF and PT values in this test system, requiring PF 50 W to calibrate Qt.

Qt can be calculated according to formulas (1) and (2). The following equations are obtained for (1) and (2) [15, 16]:

$$E_{acc} = \sqrt{\frac{4 \cdot r/Q \cdot Pf \cdot Qe}{L}}$$
$$E_{acc} = \sqrt{\frac{r/Q \cdot Pt \cdot Qt}{L}}$$

where L is the effective acceleration length of the cavity, r/Q is the cavity geometric factor, and Qt is the loaded quality factor. According to Eq. (3), Qhomc and Qhompu are calculated. For the strongly coupled cavity, according to Eq. (4) and (5):

$$Qe \ll Q0, Qt, Qhomc, Qhompu$$

where f0 is the cavity resonance frequency and τ is the cavity decay time. The total module voltage is calculated as (7):

$$Vc = \sum_{n=1,2,3\ldots 8} (Eacc_n) \cdot L$$

The RF test schematic diagram is illustrated in Fig. 5 [FIGURE:5]. The frequency of each cavity is measured by a frequency counter, while the power value of each cavity is measured by power meters. τ is obtained from the LLRF SEL loop and calculated from the PT decay time. To reduce the number of power meters and frequency counters, a seven one-eighths RF switch controller is used to switch the power of the HOM port, as well as the cavity PF/PT frequency, spectrum, and oscilloscope. The 3.9 GHz module in HTF4 is shown in Fig. 6

.

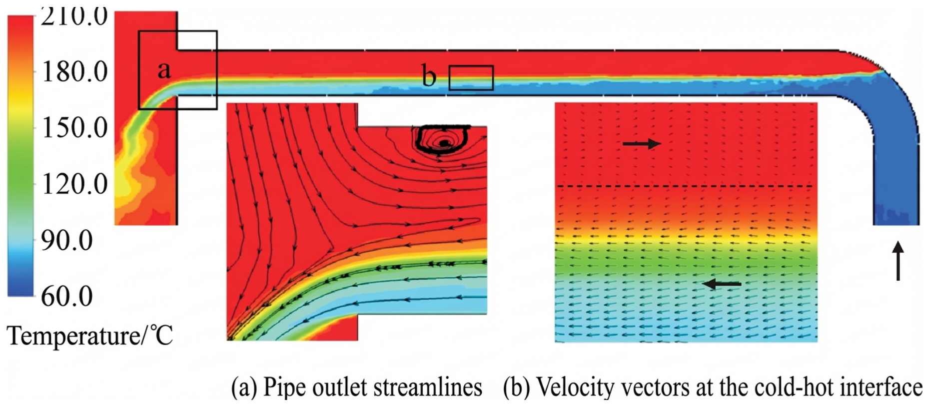

Figure 3: Figure 6

III. SOFTWARE IMPLEMENTATION

A. Software Architecture

In this system, an SNMP agent is applied on each device to collect data and respond to requests from the SNMP manager that runs on both the device and the IOC server [17]. Time synchronization is achieved using the Network Time Protocol (NTP), while Management Information Bases (MIB) [18] are used to query device status information and return it to the SNMP manager. The SNMP acquires these response data and maps them to process variables (PV) in the real-time database (db) file. These PVs are accessed and visualized through the operator interface (OPI), developed with PyDM and connected via the Channel Access (CA) protocol [19]. In addition, PV data can be retrieved from the Archiver Appliance through its HTTP interface for historical data storage and retrieval. The software architecture of the RF test system is illustrated in Fig. 7

, and the SHINE archiver is shown in Fig. 8 [FIGURE:8].

B. Device Control

StreamDevice is an EPICS support module designed for devices with byte-stream communication interfaces. It incorporates an asynDriver interface to handle underlying communication protocols [20, 21] and can be extended to support additional bus drivers. In the RF test system, multiple devices are integrated, including: (1) ROHDE&SCHWARZ N8PRS power meter (USB 3.0 interface); (2) KEYSIGHT 53230A frequency counter (Ethernet interface); (3) RF switch controller (Ethernet interface); and (4) KEYSIGHT EXA spectrum analyzer (VNC server interface). Except for the spectrum analyzer, which uses VNC for communication, the other devices are controlled through StreamDevice. The StreamDevice protocol uses plain ASCII text to execute commands

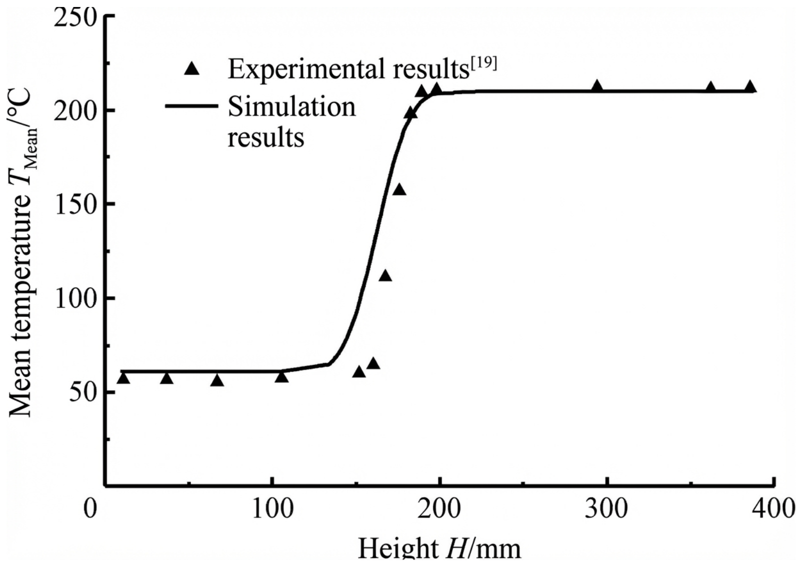

Figure 4: Figure 7

during IOC startup, with protocol files written based on hardware control commands. An example of a power meter driver configuration is as follows:

```
terminator = CRLF;
ReplyTimeout = 1000;
ReadTimeout = 1000;
Separator = ",";

reset {
    out "*rst";
}

start {
    out "INIT: CONT %d";
}

getpower {
    ExtraInput = Ignore;
    out "FETCH?";
    in "%f";
}
```

C. Data Acquisition and Storage

Data acquisition is carried out using the EPICS real-time database, which communicates with the device layer over the network to enable data collection and storage. Upon request from the OPI client, real-time data are transmitted and displayed. The data are stored in database files [22, 23]. An example of a real-time database record file is shown below:

```
record (ao "(DEV) powermeter")
field (DESC, "set off value(dB)")
field (EGU, "W")
field (SCAN, "Passive")
field (DTYP, "stream")
field (VAL, "1")
field (OUT, "@simple.proto setoffset (POW-port)")
```

In this configuration, the DESC field describes the signal name, the EGU field specifies the engineering unit, the DTYP field declares the device type, and the SCAN field determines the scanning interval. The minimum period is set to 0.1 seconds to ensure accurate data acquisition and display. To improve reusability, the database file employs macro replacement. For example, (DEV) identifies the device, and (POW-port) loads specific parameters through the dbLoadRecords command in the IOC startup script. Historical data storage is implemented using the Archiver Appliance, which archives millions of PVs from all systems. During module tests, real-time PV data are archived by PV name, ensuring long-term accessibility and enabling test reports to be generated from stored data.

D. User Interface

PyDM is a PyQt-based framework for developing user interfaces in control systems. It supports both a drag-and-drop screen builder for simple applications and a Python-based framework for building complex interfaces [24, 25]. The combination of Qt's cross-platform features and Python's flexibility makes PyDM effective for operator interfaces in EPICS environments. The OPI for Test Hall 1 is presented in Fig. 9

.

The user interface of the RF test system is divided into four sub-interfaces based on operational and display functions: (1) Sub-interface 1 displays cryogenic parameters, RF parameters, radiation parameters, vacuum parameters, and dark current parameters; (2) Sub-interface 2 provides tools for superconducting cavity calibration; (3) Sub-interface 3 supports channel selection on the 1-in-8 RF switch, oscilloscope monitoring, data saving for cavities and couplers, and calibration of the power meter; and (4) Sub-interface 4 configures measurement settings such as power meter functions, time and pulse points, and startup/shutdown control of devices. The OPI for RF test sub-1 is shown in

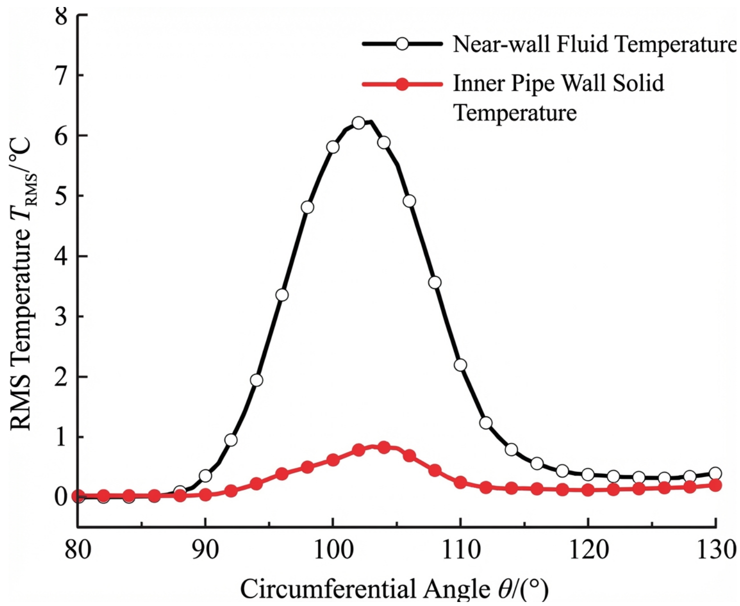

Figure 5: Figure 9

Fig. 10

, sub-2 in Fig. 11 [FIGURE:11], and sub-3 in Fig. 12 [FIGURE:12].

E. Time Synchronization

Time synchronization requirements depend on the experiment [26]. High-precision applications require nanosecond accuracy, whereas millisecond precision is sufficient for module testing. NTP [27], a TCP/IP application-layer protocol, is widely used to synchronize clocks between clients and servers. A dedicated NTP server provides synchronized system time. Timesyncd is adopted instead of NTP in the RF test system. Timesyncd connects to the same time server within the Ubuntu operating system, offering a lightweight and well-integrated solution for millisecond-level synchronization. The NTP server configuration for timesyncd is located at `/etc/systemd/timesyncd.conf` [28].

IV. TEST AUTOMATION

Automation scripts are written in Python with PyDM-based interfaces for three primary functions:

A. Cavity Tuning Automation

The program automatically determines the phase difference of the cavities, enabling simultaneous tuning of eight cavities in π-mode. The cavity tuning proce-

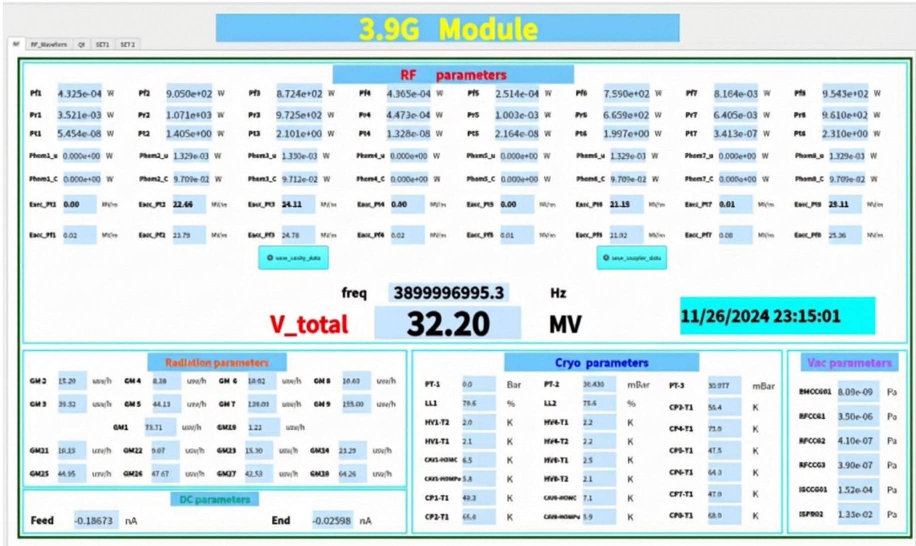

Figure 6: Figure 10

dure consists of two stages. First, coarse tuning is performed in 10° increments to locate the maximum value of PT. Then, fine-tuning is carried out in 0.1° increments within a $±$3° range around the resonance point to accurately confirm the resonance phase by identifying the peak value of PT. The flowchart of the tuning process is shown in Fig. 13 [FIGURE:13], and the user interface is presented in Fig. 14

.

B. FPC Automatic Conditioning System

Each FPC must be conditioned both at room temperature and at 2 K in the detuning cavity. Conditioning at room temperature is divided into pulse and CW modes, while conditioning at 2 K must be performed in CW mode. A Python script automates this process, with the interface implemented in PyDM. For pulse conditioning, the power is increased from 10 Hz and duty cycle from 5% to 20%. For CW conditioning, the power is raised from 500 W to 4 kW in 500 W increments, with each step maintained for 30 minutes. Conditioning is completed at 4 kW when either the temperature of the coupler's cold section reaches 323 K at room temperature, or the temperature rise of the cold section at 2 K is less than 0.1 K within 1 hour. The process flowchart is shown in Fig. 15 [FIGURE:15], and the OPI is presented in Fig. 16

.

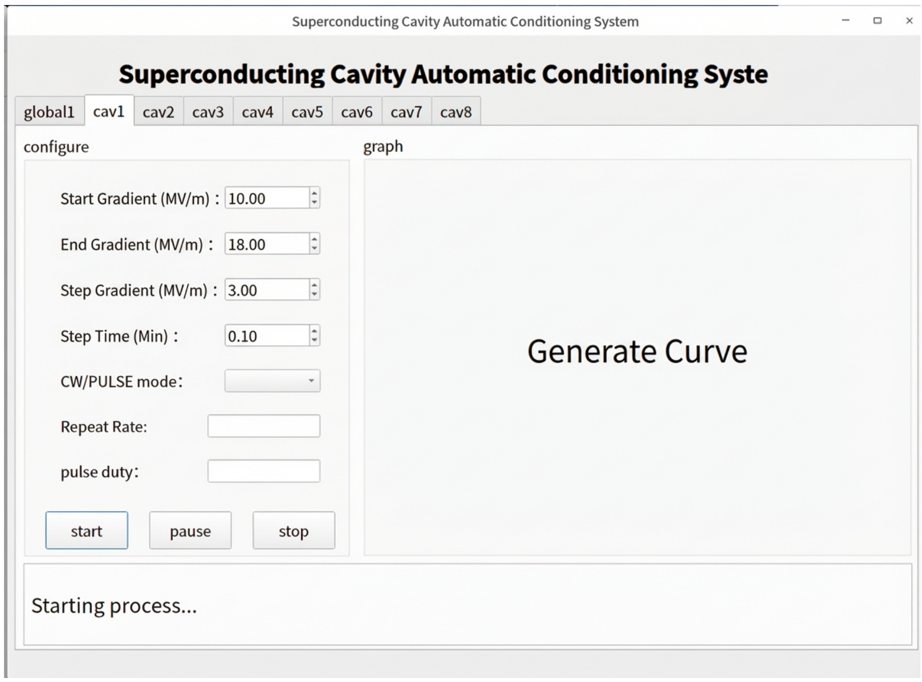

Figure 7: Figure 14

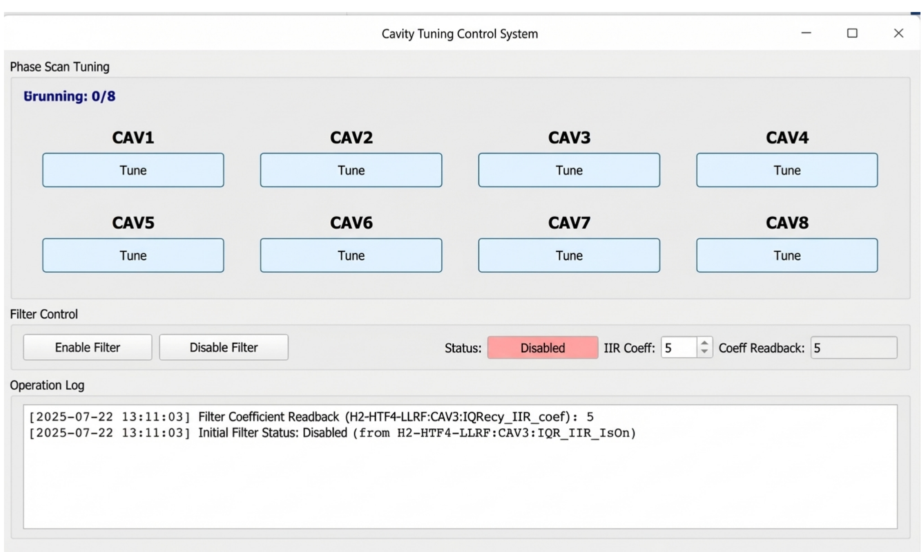

Figure 8: Figure 16

C. Cavity Automatic Conditioning System

The cavity conditioning process is carried out using a Python script, with the user interface built with PyDM. The procedure starts at 16.5 MV/m and progresses to 26 MV/m in 0.1 MV/m increments, with each step held for 2 minutes. When cavity quench [32] occurs, the automation system resets the interlock and SSA. If another interlock occurs, the automatic program quits and an audible alert is triggered. The automatic system increases Eacc to its usable level in less than two hours. The user interface is presented in Fig. 16

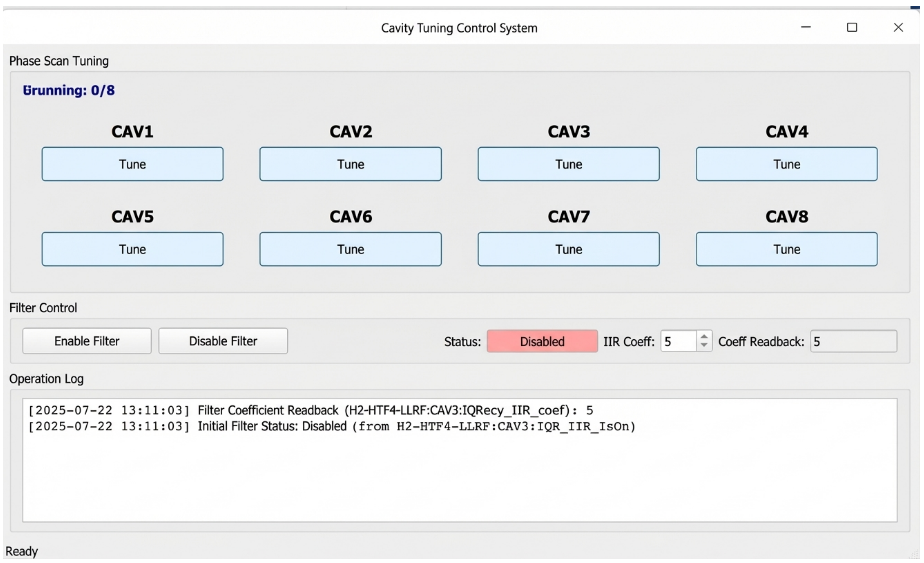

Figure 9: Figure 16

, and the result of cavity automation conditioning for CAV2 is illustrated in Fig. 17 [FIGURE:17].

V. CONCLUSION

In this work, we presented the development of an EPICS-based test system for the SHINE module. To date, more than 20 superconducting modules have been successfully tested in this system. For the 3.9 GHz modules, the results are: Vc > 36 MV, Q0 > 2E+9 @ 36 MV. For the 1.3 GHz modules, the results are: Vc > 166 MV for all modules except CM10, and Q0 > 3E+10 @ 166 MV for all modules except CM2 when MP quenches occurred before Q0 testing. All modules, including i1CM, i8CM, 3.9 GHz, and 1.3 GHz modules, have been tested in ATF1 and ATF2. The i1CM and i8CM have been installed in the injector section, which achieved 100 MeV on October 30, 2024 [33]. The CM1, CM2, and 3.9 GHz modules have been installed in the L1 section, where beam commissioning is ongoing. The CM3–CM15 are currently being installed in the

L2 section.

Automation dramatically enhanced the efficiency and standardization of the procedure. Cavity conditioning tests showed that a complete performance evaluation, which previously required 72 hours of continuous manual operation, is now executed autonomously in approximately 28 hours, representing a 61% reduction in testing time and a significant decrease in operational labor costs. The upgraded automated test system has demonstrated that automation yields a dramatic improvement in accuracy and repeatability, which is critical for the quality control of SHINE's large-scale module deployment. Future work will focus on integrating data analysis [34] and predictive maintenance algorithms into the control loop to further optimize the operational efficiency and reliability of the test facility.

VI. BIBLIOGRAPHY

Acknowledgments

We thank the RF, cryogenics, LLRF, vacuum, mechanical, electronics, and radiation-safety teams for on-site support during all module tests, and the control team for maintaining EPICS and Archiver Appliance. We also acknowledge the partner company for its efforts in testing time and data collection.

[1] C. Feng, H.X. Deng, Review of fully coherent free-electron lasers. Nucl. Sci. Tech. electron https://doi.org/10.1007/s41365-018-0490-1 (2018).
[2] Y.W. Gong, M. Zhang, W.J. Fan, et al., Beam performance of the SHINE dechirper. Nucl. Sci. Tech. 32(3), 29 (2021). https://doi.org/10.1007/s41365-021-00860-8
[3] J.F Chen, B Liu, D Wang, et al. Cryomodules development for SHINE project, https://doi.org/10.18429/JACoW-IPAC2024-WEPS42
[4] H.T. Hou, J.F. Chen, et al. Prototypes Fabrication of 1.3 GHz Superconducting RF Components for SHINE Project, https://doi.org/10.18429/JACoW-SRF2019-MOP049
[5] PSI StreamDevice Software Documentation. Available: http://epics.web.psi.ch/software/streamdevice (accessed Aug. 2025).
[6] Argonne National Laboratory, EPICS – Experimental Physics and Industrial Control System. 2021-02-28. Available: https://epics.anl.gov (accessed Aug. 2025).
[7] F. Schölz, C. Adolphsen, J. Carwardine, et al. Cryomodule testing for LCLS-II. Proc. SRF2017 [C], Lanzhou, China, 2017, pp. 747–751. https://doi.org/10.18429/JACoW-SRF2017-THPB030
[8] C. Pagani, P. Pierini. Testing of superconducting RF cavities and cryomodules for particle accelerators. Supercond. Sci. Technol. 30, 023001 (2017). https://doi.org/10.1088/1361-6668/30/2/023001
[9] Z.Y. Ma, S.J. Zhao, et al. Ultra-high quality factor and ultra-high accelerating gradient achievements in a 1.3 GHz continuous wave cryomodule. Nucl. Sci. Tech. 36, 2 (2025). https://doi.org/10.1007/s41365-024-01630-y

[10] Z.Y. Ma, S.J. Zhao, et al. High RF power tests of the first 1.3 GHz fundamental power coupler prototypes for the SHINE project. Nucl. Sci. Tech. 33, 10 (2022). https://doi.org/10.1007/s41365-022-00984-5A
[11] Branlard J. Low-level radio-frequency systems for accelerators. Nucl Instrum Methods Phys Res A, 768: 98–108, 2014.
[12] Q. Ma, L. Wang, J. Yang, and Y. Li, "Cryogenic system for superconducting radio frequency cavities," Nucl. Sci. Tech, vol. 31, no. 11, p. 111, 2020, http://doi.org/10.1007/s41365-020-
[13] L. Wang, Q. Ma, Y. Li, and J. Yang, "Dynamic heat load measurement of a superconducting cryomodule," Nucl. Sci. Tech, vol. 29, no. 9, p. 109, 2018, http://doi.org/10.1007/s41365-018-
[14] W. Pan, R. Ge, M. Li et al., Cryogenic system of the high performance 1.3 GHz 9-cell superconducting radio frequency prototype cryomodule. Appl. Thermal Eng. 255, 124042 (2024). https://doi.org/10.1016/j.applthermaleng.2024.124042
[15] Padamsee H, Knobloch J, Hays T, et al. RF superconductivity for accelerators[M]. New York: John Wiley, 1998.
[16] Hasan Padamsee. Superconducting Radio-Frequency Cavities [M]. Weinheim: Wiley-VCH, 2008.
[17] J. Case, M. Fedor, M. Schoffstall, J. Davin. A Simple Network Management Protocol (SNMP). RFC 1157, IETF, 1990. Available: https://www.rfc-editor.org/rfc/rfc1157
[18] K. McCloghrie, M.T. Rose. Management Information Base for Network Management of TCP/IP-based Internets: MIB-II. RFC 1213, IETF, 1991. Available: https://www.rfc-editor.org/rfc/rfc1213
[19] M. Davidsaver, A. Johnson, E. Norum, et al. EPICS: Evolution and future directions. In: Proc. ICALEPCS, Barcelona, Spain, 2011, pp. 293–296 [C]. https://doi.org/10.18429/JACoW-ICALEPCS2011-MOAOB01
[20] StreamDevice: General purpose device support for devices with a byte stream based communication interface. Paul Scherrer Institute, Switzerland. Available online: https://paulscherrerinstitute.github.io/StreamDevice/ (accessed 20 Aug 2025).
[21] Zimoch D. StreamDevice – a device support module for communicating with devices via ASCII-based protocols. In: Proc Int Conf Accelerator and Large Experimental Physics Control Systems (ICALEPCS 2003), Gyeongju, Korea, 2003.
[22] L.R. Dalesio, M.R. Kraimer, A.J. Kozubal. EPICS architecture. In: Proc. ICALEPCS, Berlin, Germany, 1991, pp. 278–282 (2018).
[23] Z.L. Zhao, H.C. Xu, P.R. Gong. Beamline data management system based on Archiver Appliance. Nucl. Tech. 41(3), https://doi.org/10.11889/j.0253-3219.2018.hjs.41.030102 (in Chinese).
[24] Dalesio, M. Davidsaver, M. Clausen, et al. PyDM: Python Display Manager for Control Systems. In: Proc. ICALEPCS, Barcelona, Spain, 2017, https://doi.org/10.18429/JACoW-ICALEPCS2017-TUPHA093
[25] SLAC Laboratory. PyDM – Python Display Manager. 2022-11-17. Available: http://slaclab.github.io/pydm/index.html
[26] M.Q. Zeng, L. Yin, C.C. Yin, et al. Development and implemen-

tation of an EPICS-based timing equipment control system for SHINE beamlines and endstations. Nucl. Sci. Tech. 46(7), 070102 (2023). https://doi.org/10.11889/j.0253-3219.2023.hjs.46.070102 (in Chinese).
[27] D.L. Mills. Network Time Protocol (NTP), Version 3: Specification, Implementation and Analysis. RFC 1305, IETF, 1992. Available: https://www.rfc-editor.org/rfc/rfc1305
[28] Ubuntu. timesyncd.conf– Network Time Synchronization Configuration [EB/OL]. Available: https://manpages.ubuntu.com/manpages/timesyncd.conf (accessed Aug. 2025)
[29] H. Weise. European XFEL superconducting RF gun and cryomodule tests. Nucl. Instrum. Methods Phys. Res. A 768, 1–6 (2014). https://doi.org/10.1016/j.nima.2014.09.051
[30] A. Gurevich, "Multipacting, RF heating and other mechanisms of surface resistance in superconducting radio frequency cavities," Rev. Accel. Sci. Tech. 5, (2012). https://doi.org/10.1142/S1793626812300063
[31] TESLA Collaboration. TESLA Technical Design Report, Part II: The Accelerator. DESY 2001-011, Hamburg: DESY, 2001.
[32] S. Posen, A. Cravatta, et al. "High energy gradient quench behavior verification in continuous wave accelerator," Phys. Rev. Accel. Beams 25, 042001. https://doi.org/10.1103/PhysRevAccelBeams.25.042001
[33] Hard X-ray free-electron laser device injector achieves 100 MeV beam acceleration. http://www.sari.cas.cn/news/ttxw/202504/t20250425_{7615991}.html
[34] MySQL. https://www.mysql.com/ (accessed Aug. 2025).